J. E. Unruh*
E. M. Mikhail
School of Civil Engineering
Purdue University
West Lafayette, IN 47907

Mensuration Tests Using Digital Images†

No strong dependence on pixel size seems to exist as long as pixels are 50 μm or smaller.

Introduction

Digital images are slowly becoming more common in the photogrammetric community. Sometimes images are acquired in digital form as, for example, multispectral scanner images. At other times, photographs may be digitized to permit digital image processing or for image transmission. Whether originally digital or digitized, analog presentations of digital image files on film (which are called digital images) typically contain a distinct block structure associated with individual picture elements or pixels. The main objective of this paper is to determine the effect of such structure, if any, on mensuration tasks.

Two experiments, which examine how various parameters characteristic of digital images affect the capability to photogrammetrically exploit them, are described. In one experiment a stereopair of photographs having reseau grids was digitized and reimaged several times. The reseau intersections were measured monoscopically and stereoscopically on both the original images and derived digital images. In the second experiment a series of digitally synthesized aerial photographs were measured in order to evaluate the case of having originally digital images.

Abstract: *Digital image files were written on photographic film using 25, 50, and 100 micrometre pixels. The resulting images were then measured monoscopically and stereoscopically. Measurement precisions associated with images having 25 and 50 micrometre pixel sizes were comparable. 100 micrometer pixel size had an adverse effect on measurement precision.*

Mensuration of Digitized Photographs

Two overlapping mapping-quality aerial photographs taken near Phoenix, Arizona were selected for the experiment. A test area was then identified on both photographs. The test area is about 8 by 8 cm square on each photograph.

The test area on each photograph was digitized three times with scanning apertures of 12.5, 25, and 50 μm, respectively, using an Optronics drum microdensitometer. Following digitization, each digital image file was reimaged using the same Optronics device. Images digitized at 12.5 and 25 μm were reimaged at 25 μm pixels, while the 50 μm digitized data were reimaged with 50 μm pixels. Hence, the written images ranged in scale from 2:1 to 1:1 compared to the original image. The selection of scanning and reimaging apertures was dictated by the Optronics equipment. The equipment digitizes at 12.5, 25, and 50 μm and writes at 25, 50 and 100 μm.

The results of this process were four sets of stereo pairs. The original photographs are referred to as the host images, *H*. The three sets of stereo pairs digitized at 12.5, 25, and 50 μm are referred to as *A*, *B*, and *C*, respectively.

Each reseau mark was a cross constructed from perendicular line segments about 20 μm wide on

* With the Defense Mapping Agency Aerospace Center, St. Louis AFS, MO 63118.

† Presented paper, Commission III, 14th Congress of the International Society for Photogrammetry, 13-25 July 1980, Hamburg, Federal Republic of Germany.

Photogrammetric Engineering and Remote Sensing,
Vol. 48, No. 8, August 1982, pp. 1343-1349.

0099-1112/82/4808-1343$02.25/0

the host imagery. The marks were arranged in rows spaced one centimetre apart. Along rows, the spacing was also one centimetre. Additionally, marks were offset from row to row by a half centimetre, giving the grid a staggered or skewed appearance. Each of the two images of the test area contains 64 (8 rows and 8 columns) reseau intersections, which were used for measurements. It should be noted that the reseau intersections cannot be viewed in stereo.

All the measurements, both monoscopic and stereoscopic, were made by a single person using a Bendix AS-11B-1 Analytical Stereoplotter. The observer was a photogrammetrist skilled in the use of the plotter. No specific pointing procedures were imposed on the observer.

Monoscopic Reseau Intersection Measurements

The measurements were first screened for blunders. We will denote the left and right images of each pair by the subscripts 1 and 2, respectively. Following this screening, there were measurements for the following reseaus: 63 on images A_1 and A_2, 61 on image B_1, 62 on image B_2, 29 on C_1, and 39 on C_2. The reduced amount of data for images related to stereopair C (the 50 μm case) resulted from the circumstance that many of the reseau intersections were so degraded that they could not be measured. This degradation was expected because the 50 μm quantization aperture was more than twice the width of the reseaux.

Coordinates measured on the digitized images were then transformed into the measurement coordinate system of the corresponding host image. A linear affine model was used for this purpose. This model was selected because it compensates for a slight rectangularity present in digital image pixels as well as a slight skewing caused by small systematic errors in alignment of adjacent rows of pixels.

The x residuals from the adjustment of A_1 to H_1 were combined with the x residuals from the adjustment of A_2 to H_2 and a sample standard deviation was computed. A similar procedure was performed for the y residuals. Likewise, the same computations were performed for B to H and C to H. These results are shown in Table 1 under the heading "Pooled Standard Deviation."

The pooled standard deviations contain the combined noise from host and digitized image measurements. Because of the constraint on image orientation which was enforced prior to measurement, these noise components are expected to combine according to the model shown as Equation 1. In the equation σ_P is the pooled standard deviation, σ_H is the standard deviation of the host image measurements, S is the adjustment scale factor (shown in Table 1), and σ_D is the standard deviation of the digitized image measurements. The equation may be applied to either coordinate, i.e.,

$$\sigma_P^2 = \sigma_H^2 + S^2\sigma_D^2 \qquad (1)$$

The available data do not permit the pooled standard deviation to be reliably factored into the desired components. However, photogrammetrists who have experience measuring similar reseau grids estimate that $\sigma_x = 5$ μm and $\sigma_y = 8$ μm might be expected for the host image measurements. With this information, Equation 1 was used to estimate the standard errors for the digitized image measurements shown in Table 1.

The data show no strong dependence between measurement precision and pixel size. If precisions for the host image measurements were correctly estimated, the measurements on digitized images were three or four micrometres noisier than the host image measurements. The added noise could be caused by pixel structure or by other factors, such as photo read and photo write distortions, film distortions, and reduced image resolution. In the authors' judgement, the other factors present more plausible explanation for any additional measurement noise in the digitized images than the pixel structure factor.

Stereo Measurements

Stereoscopic measurements were also made on the host pair and on digitized pairs A and B. Stereo measurements from pair C, while desirable, were not obtained for lack of time.

Once a stereo model was established, the observer visited a preselected reseau intersection on

Table 1. Precision Data for Monoscopic Measurement

Adjustment Sampling By Stereopair			Scale	Pooled standard factor Deviation		Est. std. dev. for digitized image	
	Read (μm)	Write (μm)	# (S)	σ_x (μm)	σ_y (μm)	σ_x (μm)	σ_y (μm)
A-H	12.5	25	½	6	12	7	15
B-H	25	25	1	8	13	6	10
C-H	50	50	1	12	13	11	11

photograph 1 of the pair. The measuring marks were then positioned "on the ground" at the reseau intersection and the model coordinates were recorded. On the host pair a total of 31 sets of model coordinates were collected this way (every other reseau intersection was measured to conserve instrument time). Prior to removing the images from the plotter, the instrument settings were recorded so that the stereo-model could be reestablished.

The plan was to use the established instrument settings for the host pair also with the digitized stereopairs. In this way, all measurements would be referenced to the same coordinate system. However, because of distortions in the digitized images (differential x-y scaling and non-perpendicularity), the models formed in this manner were not parallax free. Therefore, the instrument settings for each digitized stereopair had to be adjusted slightly. As a result, slightly different model coordinate systems were established for each stereopair of photographs.

Because each of the three sets of stereo measurements were in slightly different coordinate systems, a three-dimensional similarity transformation was performed in order to bring the model coordinates for the digitized images into registration with coordinates from the host stereo-model. All applicable model coordinates were used in these transformations. The calculated transformation residuals showed systematic trends in the horizontal components which are characteristic of scale errors. After some investigation, the observed systematic trends were linked to the known rectangularity of pixels which is characteristic of the digitized imagery. The corrections were applied to the residuals to remove the trends.

Sample standard deviations computed using the trend corrected residuals are shown in Table 2. Experimental variation of quantization levels between Models *A* and *B* did not significantly affect the observed precision measures.

Mensuration of Synthetic Photographs

The second experiment involved the measurement of synthetic aerial photographs. The image synthesis capability, described by Mikhail *et al.* (no date, 1977), was used in the following manner. An orthophoto of an area (approx. 5.3 km by 8.3 km) near Ft. Sill, Oklahoma, was digitized using a sample interval of 4.8 m on the ground. Then each pixel in the digital orthophotograph was associated with an elevation value from a specially prepared digital terrain elevation model. The combined elevation and image data were then processed using the photograph synthesis computer programs to construct digital image files having the desired perspective geometry. This process is analogous to inverse digital orthophoto production. Synthetic photographs generated in this manner have the desirable properties that object space is perfectly known and that image geometry is subject to rigid control.

For this experiment, digital image files for three stereopairs of synthetic photographs (A, B, & C), of the Ft. Sill site were constructed. Each stereo model imaged the same terrain and had a base-to-height ratio of 0.69. All photographs are perfectly vertical relative to the horizontal datum. The three sets of files were different from one another in resolution. The average ground separation between adjacent image pixels was 2.4 metres, 4.8 metres, and 9.6 metres for photographs of stereopairs A, B, and C, respectively. Each digital image file was then written three times to film (Optronics accepts only film) using the three different pixel sizes of 25 μm, 50 μm, and 100 μm to yield a total of nine synthetic stereo digital images. These test photographs are described in Table 3.

Two types of targets were placed in the synthetic photographs to facilitate measurement. One type of target was a cross-shaped figure "painted" on to the digital terrain. Figure 1 shows the marking scheme. Since control point markings were processed through the synthesis algorithm as ordinary ground surface features, this marking method is analogous to paneling control points derived by ground survey prior to flying mapping photography. Since interior and exterior orientation of synthetic images is defined and therefore

Table 2. Precision Data for Stereoscopic Measurement

Residual Source	Sample Standard Deviations σ_x (μm)	σ_y (μm)	σ_z (μm)
Tranformation From-To			
A-H	11	12	13
B-H	12	12	16

Table 3. Synthetic Stereo Photography for Mensuration

Stereo Pair	Pixel Size (μm)	Photograph Resolution* (metre)	Photograph Scale
A100	100	2.4	1:24000
A050	50	2.4	1:48000
A025	25	2.4	1:96000
B100	100	4.8	1:48000
B050	50	4.8	1:96000
B025	25	4.8	1:192000
C100	100	9.6	1:96000
C050	50	9.6	1:192000
C025	25	9.6	1:384000

* Average ground Distance separating adjacent pixel centers.

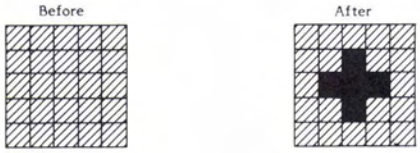

FIG. 1. Ground model modification scheme for marking control points (each square represents a brightness value stored in the ground description).

precisely known, accurate image coordinates can be computed directly from the recorded control coordinates. In general, the computed image coordinates do not coincide with image pixel centers, thus realistically representing the case of direct digital images of terrain targets. The other targets were specially darkened pixels on photograph two of the stereopairs. These targets are analogous to artificially (or PUG) marked points. The image space and object space coordinates of each target were recorded during image synthesis and may be regarded as perfectly known.

The targets were placed to fall on flat and sloping terrain as well as on image areas with both sparse image detail and plentiful image detail. Additionally, two settings of viewing magnification were used in the measuring process. These four descriptive factors were associated with targets. These factors are summarized in Table 4. In all, 32 targets were defined on each stereo pair, two targets of each possible combination of Target Factors. By design, the same targets have the same ground location in each stereopair. In this sense, the same targets appear in each stereopair.

Table 4. Target Factors.

Three photogrammetrists measured the identified targets on each of the stereo pairs using OMI-Nistri TA3P stereocomparators fitted with 30-μm measuring marks. The measuring marks cover a constant 30-μm diameter on the film stages independently of viewing magnification. In all, 864 target measurements (32 targets/stereopair $\times$ 9 stereopairs $\times$ 3 observers each pair) were collected.

All measurements associated with a single stereopair by an observer were executed in a measuring session. Sessions were constrained to begin and end in the same work shift. Each observer conducted nine sessions, one for each of the nine stereopairs.

TABLE 4. TARGET FACTORS

Factors	Level 1	Level 2
1.Target Type	single pixel target	cross target
2. Relief	flat terrain	sloping terrain
3. Contrast	sparse image detail	plentiful image detail
4. View Magnification	7×	14×

At the beginning and end of each measuring session, four or five specially marked "fiducial" pixels were measured on each synthetic photograph. These fiducial measurements were used to establish the transformation from the comparator coordinate system to the image coordinate system. The redundant measurements were also used to confirm stability of the comparator setup during the measuring session as well as precision associated with centering the measuring mark on selected pixels.

Each of the 32 selected targets were stereoscopically measured in each session. The execution of a single stereo measurement was a relatively complex process which produced five separate sets of x, y coordinates. First, the measuring mark associated with photo 2 of the pair was monoscopically centered on the target to be measured. Once this was accomplished, the stage for photo 2 remained fixed for the remainder of the measurement sequence. Next, the measuring mark for photo 1 was positioned using *stereo perception* to position the mark "on the ground" and the stage coordinates (for both comparator stages) were recorded. Photo 1 measuring mark was moved off target and repositioned, and the stage coordinates were again recorded. Then, dove prisms in the optical train were adjusted so that the imagery appeared in pseudo stereo. The photo 1 measuring mark was positioned again "on the ground" and the stage coordinates were recorded. Finally, the photo 1 measuring mark was decentered and recentered, and the stages coordinates were again recorded. Thus, one x, y coordinate pair was recorded for each point on photo 2 and four x, y coordinate pairs recorded the stereo transfer to photo 1.

All measurements were transformed into the camera system and then analyzed for measurement accuracy and precision. Accuracy measures reflect the agreement between measured target coordinates and target coordinates which are a priori known from image synthesis. Precision indicates repeatability either by a single observer or between observers.

Each fiducial pixel was measured twice by each observer. These measurements were analyzed for precision associated with centering on a pixel by a single individual. An average precision (68 percent confidence level) of 2.6 μm in either the x or y coordinate component was found to best estimate this quantity. Factors such as pixel size, the observer, the coordinate component (x, y), and comparator stage were found to have no significant effect on measurement precision.

Pixel size and target type were found to significantly affect the precision and accuracy of monoscopic measurements. Table 5 shows accuracy and precision values as a function of target type for

each monoscopically measured synthetic photograph. Additionally, pooled accuracy and precision figures for digital images with 100-μm pixels and smaller pixels are shown. The accuracies are the result of root-sum-squared computations from measurement errors. Precisions were computed by introducing a mean error (measurements by three observers) correction at each target.

Precision for single pixel targets measure the repeatability between different observers associated with centering on a pixel. The precision value for the x component is significantly larger than that associated with an observers ability to repeat himself.

The accuracy values for the single pixel targets reflect measurement precision plus errors introduced by film distortion and metric infidelity associated with the photo write device. These additional error sources are particularly significant when 100-μm pixels are used. A probable explanation for this result is that the photo write device introduced significant distortions when used to produce 100 μm pixels.

Measurements of the larger sized cross targets have lower precisions and accuracies than for single pixel targets. Measurement precision is particularly low for crosses on the 100-μm pixel-sized images.

Accuracy and precision data were also computed for measurement by stereo transfer to photograph one of the stereopair. These data are shown in Table 6. The most evident fact associated with the data is that, not unexpectedly, much more noise is associated with the process of stereo transfer than that of monoscopic pointing. The second most significant result is that target type affects precision differently in stereo transfer than in monoscopic pointing. We should note that the single pixel targets did not appear in stereo. Therefore, observers had to rely on unrelated image detail in the neighborhood of the target in order to position the measuring mark. On the other hand, cross targets, like other ground detail, were imaged on both photographs and viewed in stereo. For this reason the large noise component is associated with single pixel targets rather than the cross targets. Measuring precision associated with cross targets is essentially the same in both monoscopic and stereoscopic measurement, but precision associated with stereo transfer for single pixel targets is much lower than either stereo transfer with cross targets or monoscopic measurement of the single pixel targets.

Each target was also associated with levels of the four factors shown in Table 4. Except for target type, these factors did not greatly affect precision of monoscopic measurements. They do, however, affect precision of stereo transfer in a rather complex way. The observed precision of stereo transfer depends greatly on combinations of (interactions between) the factors as well as the factors of display resolution and pixel size. Table 7 shows some of these interactions as measured on 100-μm pixel-sized images. The 100-μm pixel was selected because the effects are largest in magnitude. Similar phenomena are present in the other images. From the table it is clear that some factor combinations are preferable to others.

In the preceding analysis, precision was expressed in micrometre units at image scale. Since synthetic photographs with a wide range of image scales were measured, precision data must be scale normalized to determine capability to extract ground information. Table 8 shows the precision data from Tables 6 and 7 normalized by simple ratio to an image scale of 1:96,000. From these data

TABLE 5. PRECISION AND ACCURACIES ASSOCIATED WITH MONOSCOPIC MEASUREMENTS OF SYNTHETIC PHOTOGRAPHS

	Single Pixel Targets				"Cross" Targets			
	Precision		Accuracy		Precision		Accuracy	
Stereopair	x (μm)	y (μm)	x (μm)	y (μm)	x (μm)	y (μm)	x (μm)	y (μm)
A (100 μm pixels)	7.5	3.9	9.1	6.5	14.2	11.9	17.7	16.4
A (50 μm pixels)	7.2	3.2	7.9	4.4	9.4	6.8	10.4	7.0
A (25 μm pixels)	5.9	3.7	13.8	4.9	5.1	4.7	12.3	4.7
B (100 μm pixels)	7.5	4.4	11.4	9.0	14.8	15.6	26.9	25.1
B (50 μm pixels)	5.2	4.6	7.4	6.6	5.5	6.4	12.0	11.6
B(25 μm pixels)	6.3	3.0	9.0	3.8	5.4	3.5	10.2	6.0
C (100 μm pixels)	7.4	5.5	32.4	8.8	20.8	4.9	35.0	19.5
C (50 μm pixels)	5.7	3.6	5.4	4.1	9.4	6.4	12.9	11.4
C (25 μm pixels)	6.6	4.3	7.6	4.5	9.0	4.0	9.4	5.4
All 100 μm pixels	7.5	4.7	20.6	8.2	16.9	11.7	27.5	20.6
All 50 × 25 μm pixels	6.2	3.8	8.9	4.8	7.6	5.4	11.3	8.2

TABLE 6. PRECISIONS AND ACCURACIES ASSOCIATED WITH STEREOSCOPIC TRANSFER USING SYNTHETIC PHOTOGRAPHS

	Single Pixel Targets				"Cross" Targets			
	Precision		Accuracy		Precision		Accuracy	
Stereopair	x (μm)	y (μm)	x (μm)	y (μm)	x (μm)	y (μm)	x (μm)	y (μm)
A (100 μm pixel)	152	91	187	101	32	15	35	20
A (50 μm pixel)	22	23	24	24	11	12	12	12
A (25 μm pixel)	13	18	13	20	6	9	7	10
B (100 μm pixel)	64	27	68	30	42	18	47	26
B (50 μm pixel)	16	9	15	12	7	10	13	14
B (25 μm pixel)	15	13	13	13	7	8	8	10
C (100 μm pixel)	40	12	45	13	26	9	31	20
C (50 μm pixel)	15	12	18	11	11	8	15	11
C (25 μm pixel)	12	10	13	10	7	8	8	11
All 100 μm pixel	98	55	118	61	34	14	39	22
All 25 $\times$ 50 μm pixel	16	15	17	16	8	9	11	11

TABLE 7. PRECISION OF STEREO TRANSFER USING DIGITAL IMAGES WITH 100-μM PIXELS AS A FUNCTION OF FACTOR COMBINATIONS

Factor 1	Factor 2	x (μm)	y (μm)	Factor 2	x (μm)	y (μm)
S P Target*	Sloping Relief	125	69	Flat Relief	60	14
Cross Target	Sloping Relief	35	37	Flat Relief	32	15
S P Target	Poor Contrast	130	76	Good Contrast	49	17
Cross Target	Poor Contrast	38	14	Good Contrast	28	14
S P Target	14× Magn.	126	70	7× Magn.	57	35
Cross Target	14× Magn.	33	13	7× Magn.	34	15
S R Target**	Poor Contrast	120.2	68	Good Contrast	49	18
Flat Target	Poor Contrast	62	37	Good Contrast	29	13
Sloping Target	14× Magn.	121	70	7× Magn.	48	20
Flat Target	14× Magn.	50	23	7× Magn.	47	32
Poor Contrast	14× Magn.	122	70	7× Magn.	56	33
Good Target	14× Magn.	47	13	7× Magn.	32	18

* Single pixel target
** Sloping relief target

TABLE 8. PRECISION DATA SCALE NORMALIZED TO 1:96000

		Normalized Monoscopic (all targets)		Precision Stereo transfer			
				Single Pixel		Cross	
Stereo Pair	Original Scale	x (μm)	y (μm)	x (μm)	y (μm)	x (μm)	y (μm)
A100	1:24000	3	3	38	23	8	10
A050	1:48000	5	4	11	12	6	6
A025	1:96000	6	5	13	18	6	10
B100	1:48000	6	6	32	14	21	13
B050	1:96000	6	6	16	9	7	14
B025	1:192000	12	7	30	26	14	20
C100	1:96000	16	6	40	12	31	20
C050	1:192000	16	10	30	24	30	22
C025	1:384000	31	17	48	40	32	44

it is clear that the ability to extract information increases with photograph resolution.

Conclusions

In summary, the experimental data presented here point to the following conclusions:

- In so far as the observer is concerned, the block structure of digital images having pixel sizes of 50 μm or smaller does not seem to interfere with pointing ability.
- In selecting a sample rate for digitization, only the capability to resolve desired image detail (mensuration targets) need be considered.
- Stereo transfer is the primary source of measurement noise.
- Noise associated with stereo transfer is related to factors of terrain relief, target type, density of image detail (contrast), and viewing magnification. Measurement precision deteriorates rapidly when unfavorable levels of two or more of these factors occur.
- The results from the experiment using digitized images are in agreement with those from the experiment using originally digital (synthesized) images in that no strong dependence on pixel size seems to exist as long as pixels are 50 μm or smaller.

The results given in this paper are the first step in a continuing research effort at Purdue University to evaluate the metric aspects of digital images. While significant findings have been found, it is our intention to confirm these results with further experiments. Not only static mensuration tasks, but also dynamic tasks, such as continuous profiling, are being investigated. Furthermore, pertinent operations in digital image processing as well as considerations of soft-copy image mensuration are planned for future work.

References

Mikhail, E. M., J. E. Unruh, and D. H. Alspaugh, no date. *Sensor Simulation from Spectral and Digital Terrain Data,* Final Technical Report, DMAAC, St. Louis, Mo., Contract No. DMA 700-75-C-0119.

———, 1977. Image Simulation from Digital Data, *Proceedings of the Fall Technical Meeting of the American Congress on Surveying and Mapping.*

(Received 30 January 1981; revised and accepted 27 December 1981)

Forthcoming Articles

O. O. Ayeni, Optimum Sampling for Digital Terrain Models: A Trend Towards Automation.
O. O. Ayeni, Phototriangulation: A Review and Bibliography.
Gérard Begni, Selection of the Optimum Spectral Bands for the SPOT Satellite.
C. B. Chittineni, Fisher Classifier and its Probability of Error Estimation.
Lionel E. Deimel, Jr., Robert J. Fornaro, David F. McAllister, and *Calvin Lee Doss, II,* Techniques for Computerized Lake and River Fills in Digital Terrain Models.
Ismat M. ElHassan, Rotary Focal-Plane Shutter Distortion.
David C. Goodrich, A Simple 35-mm SLR Photogrammetric System for Glacier Measurements.
R. D. Graetz and *M. R. Gentle,* The Relationships between Reflectance in the Landsat Wavebands and the Composition of an Australian Semi-Arid Shrub Rangeland.
G. Ladouceur, P. Trotier, and *R. Allard,* Zeiss Stereotop Modified into an Analytical Stereoplotter.
Atsushi Okamoto, Wave Influences in Two-Media Photogrammetry.
A. Prieto, J. Bescós, and *J. Santamaría,* Spatial Frequency Pseudocolor Filters.
Urho A. Rauhala, Array Algebra Estimation in Signal Processing.
George H. Rosenfield, The Analysis of Areal Data in Thematic Mapping Experiments.
Paul H. Salamonowicz, USGS Aerial Resolution Targets.
J. C. Trinder, The Effects of Photographic Noise on Pointing Precision, Detection, and Recognition.